# Pyroelectric thin films—Past, present, and future

Cite as: APL Mater. **9**, 010702 (2021); https://doi.org/10.1063/5.0035735 Submitted: 31 October 2020 . Accepted: 27 December 2020 . Published Online: 22 January 2021

🗓 Gabriel Velarde, 🗓 Shishir Pandya, J. Karthik, 🗓 David Pesquera, and 🗓 Lane W. Martin











A comprehensive resource for researchers Explore theory, methods, sources of errors, and ways to minimize the effects of errors





**RESEARCH UPDATE** APL Materials scitation.org/journal/apm

# Pyroelectric thin films—Past, present, and future

Cite as: APL Mater. 9, 010702 (2021); doi: 10.1063/5.0035735 Submitted: 31 October 2020 • Accepted: 27 December 2020 • Published Online: 22 January 2021











Gabriel Velarde, Dishishir Pandya, Dishishir Pan





# **AFFILIATIONS**

- Department of Materials Science and Engineering, University of California, Berkeley, Berkeley, California 94720, USA
- <sup>2</sup>Microsoft, One Microsoft Way, Redmond, Washington 98052, USA
- <sup>3</sup>Catalan Institute of Nanoscience and Nanotechnology (ICN2), CSIC and BIST, Campus UAB, Bellaterra, 08193 Barcelona, Spain
- <sup>4</sup>Materials Sciences Division, Lawrence Berkeley National Laboratory, Berkeley, California 94720, USA

Note: This paper is part of the Special Topic on 100 Years of Ferroelectricity—A Celebration.

- <sup>a)</sup>Formerly at: Department of Materials Science and Engineering, University of California, Berkeley, Berkeley, CA 94720, USA.
- b) Formerly at: Department of Materials Science and Engineering, University of Illinois, Urbana-Champaign, Urbana, IL 61801, USA.
- c) Author to whom correspondence should be addressed: lwmartin@berkeley.edu

# **ABSTRACT**

Pyroelectrics are a material class that undergoes a change in polarization as the temperature of the system is varied. This effect can be utilized for applications ranging from thermal imaging and sensing to waste-heat energy conversion to thermally driven electron emission. Here, we review recent advances in the study and utilization of thin-film pyroelectrics. Leveraging advances in modeling, synthesis, and characterization has provided a pathway forward in one of the more poorly developed subfields of ferroelectricity. We introduce the complex physical phenomena of pyroelectricity, briefly explore the history of work in this space, and highlight not only new advances in the direct measurement of such effects but also how our ability to control thin-film materials is changing our understanding of this response. Finally, we discuss recent advances in thin-film pyroelectric devices and introduce a number of potentially new directions the field may follow in the coming

© 2021 Author(s). All article content, except where otherwise noted, is licensed under a Creative Commons Attribution (CC BY) license (http://creativecommons.org/licenses/by/4.0/). https://doi.org/10.1063/5.0035735

### I. PHYSICS OF PYROELECTRICS

While we are celebrating 100 years of ferroelectricity in this special edition, the first known report of the pyroelectric effect dates back to more than 2000 years ago when the Greek philosopher Theophrastus observed that small particles of straw and wood became attracted to a heated pyroelectric mineral. Our physical understanding of the pyroelectric effect has evolved greatly, of course, and today, pyroelectricity is defined as the variation of the spontaneous polarization (P) as a function of temperature (T). When measured at a constant electric field (E) and stress (X), this variation gives the so-called pyroelectric coefficient  $\pi$ =  $(\partial P/\partial T)_{E,X}$ . Thus, when a polar material in a capacitor structure is subjected to a change in temperature, the change in polarization drives a current in the surrounding closed circuit or a voltage in an open circuit, both of which can be utilized. As a result, ferroelectrics (because of their strong polarization) have been widely studied as pyroelectrics and used in applications ranging from infrared

imaging/sensing to waste-heat energy conversion to electron emission.<sup>3-6</sup> Despite its widespread use, our fundamental understanding of the pyroelectric effect has remained underdeveloped compared to dielectric (*E*) and piezoelectric (*X*) effects (Fig. 1). While the underlying thermodynamics appears to be straightforward, the literature on this subject provides a rather confusing picture.

Recently, advances in epitaxial thin-film synthesis and characterization have provided researchers access to model versions of ferroelectric materials, which have ushered in deeper understanding of the limits of polarization, the role of domain walls in various responses, and more. Yet, while our understanding of dielectric, piezoelectric, and ferroelectric responses have blossomed, little progress has been made in understanding pyroelectric effects. This is, in part, due to the complexity of this effect and the challenge of accurately measuring both the temperature and the often convoluted pyroelectric response in thin films. To fully quantify and control pyroelectricity, one must understand several contributions to the overall response. The total pyroelectric response  $\pi_{total}$  can be

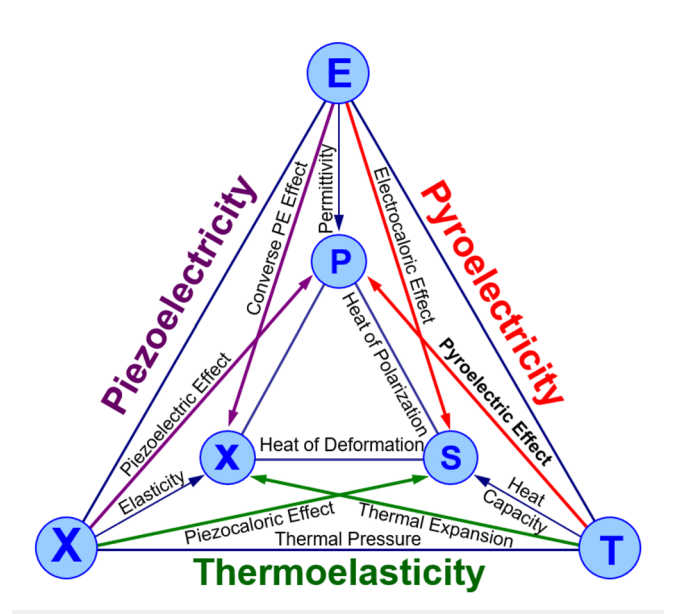


**FIG. 1.** Heckmann diagram depicting the various thermodynamic coupled electrical, mechanical, and thermal susceptibilities of crystal materials. Here, E, X, T, P, x, and S are the electric field, stress, temperature, polarization, strain, and entropy, respectively. In addition to the direct pyroelectric effect that relates polarization and temperature, other indirect thermodynamic paths are evident (e.g., pyroelectricity via temperature induced piezoelectricity).

defined as follows:

$$\begin{split} \pi_{total} &= \pi_{primary} + \pi_{secondary} + \pi_{\varepsilon} + \pi_{teriary} \\ &= \phi \bigg( \frac{\partial P}{\partial T} \bigg)_{x} + P \bigg( \frac{\partial \phi}{\partial T} \bigg)_{x} + \bigg( \frac{\partial P}{\partial X} \bigg)_{T} \bigg( \frac{\partial X}{\partial x} \bigg)_{T} \bigg( \frac{\partial x}{\partial T} \bigg)_{X} \\ &+ \varepsilon_{0} E \bigg( \frac{\partial \varepsilon_{r}(E)}{\partial T} \bigg) + \pi_{tertiary}, \end{split}$$

where  $\phi$  is the fraction of ferroelectric domains contributing to the pyroelectric response, x is the strain,  $\varepsilon_0$  is the permittivity of free space, and  $\varepsilon_r$  is the relative permittivity. Many prior studies report the primary contribution as a single value, but in reality, it is made up of a combination of both the *intrinsic* ( $\pi_{intrinsic}$ , first term) and extrinsic ( $\pi_{extrinsic}$ , second term) effects, similar to that of dielectrics.<sup>8-10</sup> The intrinsic contribution arises from the temperature dependence of P (i.e., within the ferroelectric domains), while the extrinsic contribution arises from the temperature dependence of the domain structure (i.e., thermally induced domain-wall motion).8,11 Only within the past ten years has dedicated effort been applied to elucidating the nature of extrinsic effects, specifically in thin films where deterministic control of domain architectures can be achieved. The secondary contribution ( $\pi_{secondary}$ , third term) arises from the fact that all pyroelectric materials are also piezoelectric. Thus, temperature-induced volume (shape) changes are commensurate with piezoelectric-induced polarization changes. This becomes more complex in thin films, where in-plane thermalexpansion mismatch with the underlying substrate induces additional changes in polarization via the piezoelectric effect. To encompass all these coupled subtleties, the secondary contribution includes

material properties such as the piezoelectric coefficient, elastic stiffness, and the thermal-expansion coefficient tensors. 8,12,13 Furthermore, under applied electric fields, a dielectric contribution ( $\pi_{\varepsilon}$ , fourth term) arises from the temperature and electric-field dependence of  $\varepsilon_r$ . Finally, the tertiary contribution ( $\pi_{tertiary}$ , fifth term) arises via the piezoelectric effect from inhomogeneous heating that induces nonuniform stresses.<sup>14</sup> This effect may be neglected if uniform heating is achieved, which is typically the case in thin films. To further complicate matters, each of these contributions exhibits not only various magnitudes but also varying signs depending on the nature of the system and, until recently, few attempts to measure such contributions had been undertaken. Developing methodologies to understand and quantify these complex (and competing) contributions remains a clear challenge. However, with advances in modeling and characterization, our understanding of these contributions has expanded greatly and this review aims to capture the recent history of this evolution.

# II. ADVANTAGES AND DISADVANTAGES OF PYROELECTRIC THIN FILMS

While the work on pyroelectrics is, in general, quite extensive, studies specifically on thin films are limited. Initially motivated by the enhanced performance and compatibility with the ever-shrinking dimensionality of integrated microelectronics of the time, prominent researchers (e.g., Lang, Muralt, and Whatmore) drove advances in both fundamental material understanding and commercial applications in the 1980s and 1990s. 15-17 As it pertains to thin-film pyroelectrics specifically, much early work focused on micrometer-thick micro-machined systems 15,18 for infrared sensing (Fig. 2). However, even as early as 1992, researchers at Texas Instruments, Inc. had developed uncooled infrared focal plane arrays (IRF-PAs) based on pyroelectric Ba<sub>1-x</sub>Sr<sub>x</sub>TiO<sub>3</sub> thin films with excellent performance. 19-21 This work showed the potential utility and impact of thin-film pyroelectrics and paved the way for the key developments of the past decade on nanometer-scale thin-film pyroelectric materials, which has become increasingly attractive due to the control of materials afforded by manipulating epitaxial strain, composition, thickness, and electrostatic and mechanical boundary conditions therein.<sup>7</sup> Thin films also open up the possibility of leveraging enhanced susceptibilities, low thermal mass, and microfabrication techniques for large-scale device integration, which could provide pathways to performance well beyond the theoretical limits of bulk ceramics.<sup>22</sup> Simultaneously, researchers have been developing exotic new thin-film heterostructures—from single-layer films to superlattices to compositionally graded structures—which afford previously unimagined potential for enhanced material properties. For example, large gradients in electric potential, strain, and composition can be obtained, which induce polar phenomena in thin-film devices that are simply not attainable in bulk counterparts.<sup>23</sup> Such advances have resulted in dramatic theoretical and experimental demonstrations of high efficiency pyroelectric energy conversion (PEC) and large-scale infrared detection arrays.<sup>22,24</sup>

While thin-film engineering offers a fertile opportunity for redefining the limits of pyroelectricity, it also results in significant challenges. For example, taking advantage of the new nanoscale design approaches, including utilization of thin-film strain, exotic polarization domain structures, and compositional

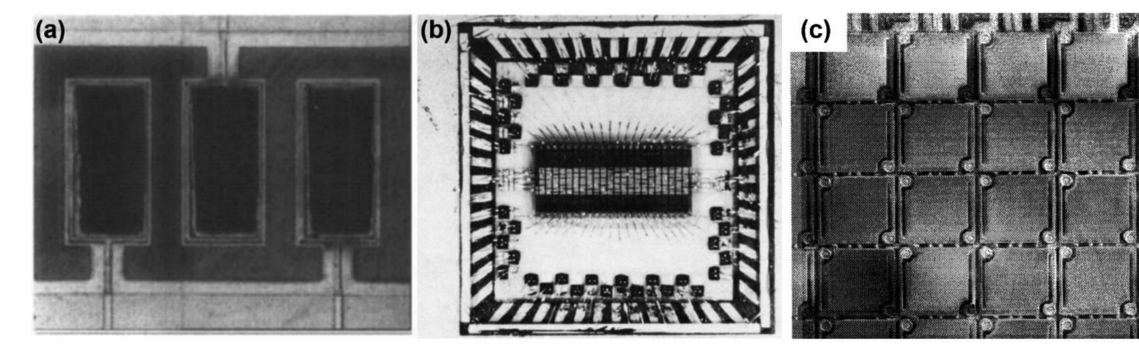


FIG. 2. (a) Three components of an early 1  $\times$  12 micromachined pyroelectric array. The 0.4  $\times$  0.9 mm<sup>2</sup> device structure consists of a 1.6  $\mu$ m-thick lead–zirconate titanate-based thin film layer capped with a black IR adsorbing platinum layer. (b) Pyroelectric linear array with two lines of lead–zirconate titanate-based active elements (black rows) capable of operating in different wavebands, thus permitting two-color IR imaging. (c) A 320  $\times$  240 pyroelectric barium–strontium titanate-based pixel array on an integrated circuit with 48.5  $\mu$ m centers. (21)

gradients, also requires advanced capabilities in thin-film growth, pyroelectric characterization, and materials modeling. The material characterization and modeling techniques that are typically suited to bulk pyroelectric materials are inadequate for thin films and provide an incomplete picture of the underlying mechanisms that impact pyroelectricity. In addition to the developed Ginzburg–Landau–Devonshire (GLD) formalisms for thin-film pyroelectrics, the development of more rigorous characterization methods has been pivotal in providing comprehensive understanding of pyroelectric response. With key advancements in the development of thin film models and characterization methods over the past decade, the 2000 year-old field of pyroelectrics now stands poised to enter the new frontier of sub-micrometer thin-film response.

# III. MEASURING PYROELECTRIC EFFECTS IN THIN FILMS

Since the 1950s, more than 20 measurement protocols have been developed taking advantage of various excitation/measurement signals and required device and material specifications (i.e., area, thermal conductivity, and specific heat capacity) that have offered varying abilities to separate out spurious effects such as thermally stimulated currents (TSCs).<sup>26</sup> The relative lack of advanced study on thin-film pyroelectrics is primarily related to the fact that direct (and accurate) measurements of applied temperature changes are difficult. The small thermal mass/area of thin-film devices and the presence of underlying substrates lead to non-trivial boundary conditions where the film loses heat to the substrate at relatively short time scales.<sup>27</sup>

### A. Direct vs indirect measurements

Pyroelectric measurements can be classified as either "direct" or "indirect" depending on how the temperature dependence of P is extracted. Direct measurements involve characterization of the temperature dependence of P directly via the pyroelectric current or voltage. In the case of a closed-circuit configuration of a parallel-plate device, the temperature stimulus and the concomitant change in P result in a flow of current through the external circuit due to a

change in the compensating charges of the electrodes. By monitoring the pyroelectric current in response to the applied temperature, the pyroelectric coefficient can be extracted directly as  $\pi = \frac{i_p}{A(dT/dt)}$ , where  $i_p$  is the pyroelectric current, A is the capacitor area, and t is the time. In contrast, indirect measurements are accomplished via multiple isothermal measurements of polarization-electric field hysteresis loops as a function of temperature. The temperature dependence of polarization  $(\partial P/\partial T)$  is then extracted to obtain  $\pi$ . Indirect measurements are simpler to implement but can lead to an overestimation of  $\pi$  due to electric-field-induced leakage currents and insensitivity to various contributions to pyroelectricity (e.g., extrinsic, secondary, or field-dependent effects), which can be particularly significant for thin films.

#### B. The evolution of direct measurements

While direct measurements offer a higher degree of accuracy, they are also more difficult to implement. Rapidly and uniformly applying temperature variations, measuring those temperature changes accurately in complex material stacks, and measuring the potentially small currents (voltages) that result from the pyroelectric effect are non-trivial. In thin films, these challenges are further exacerbated due to the reduced lateral sizes of devices (rendering thermocouple-based studies nearly impossible) and the small signal pyroelectric response itself, which can be beyond the resolution of off-the-shelf instruments. The key, however, is that the approach must be able to address potentially spurious contributions to the response, including thermally stimulated or leakage currents. Fortunately, significant work on the development of direct measurements, particularly on dynamic or phase-sensitive techniques, has incorporated microfabricated devices to overcome these metrology challenges and shed new light on the origin of pyroelectricity.

These advances, described below, build upon several important contributions to the field of pyroelectric characterization, which merit mention. Early pioneering work by Chynoweth utilized filtered tungsten projection lamps to illuminate and heat BaTiO<sub>3</sub> crystals and collect the resulting transient currents from which the pyroelectric response was extracted.<sup>28</sup> Although still limited by the

accuracy and homogeneity of the applied temperature changes, this work, unlike static methods of the time, provided a pathway whereby researchers could separate out non-pyroelectric contributions to the measured response. From here, Byer and Roundy developed a direct method that extracted the pyroelectric current using only a data acquisition system, amperemeter, and temperature-controlled oven.<sup>29</sup> While this simplicity was a step in the right direction, depending on the material and temperature regime, this approach could not fully separate out currents that were not of pyroelectric origin. In turn, Garn and Sharp applied sinusoidal temperature excitations where phase sensitivity could be maintained.30 Due to the time-derivative dependence of temperature, one can effectively separate out the true pyroelectric current (which is 90° out-of-phase with the input heating signal) from thermally stimulated currents (TSCs)31,32 that arise from thermally excited trapped charges (which are in-phase with the input heating signal). As compared to the pyroelectric current, the TSC has a large relaxation time (orders of magnitude longer than pyroelectric currents) and therefore depends more on the actual temperature and less on its time derivative. This distinguishing feature arms the pyroelectric measurement with phase selectivity during periodic (AC) heating.

# C. New approaches for thin films

Building from this idea, various studies<sup>9,30,33</sup> have employed sinusoidally oscillating temperatures and phase-sensitive measurements to extract pyroelectric currents. For example, researchers were able to apply such phase-sensitive approaches to probe pyroelectric effects in thin films by oscillating the temperature of the entire film stack (substrate and films). 9,34 The challenge in this approach was multifold but was primarily limited by the small temperature magnitudes (~1.25 K) and slow oscillations (0.125 rad/s) needed to maintain homogeneous heating. Unsurprisingly, these applied temperature variations on small device structures (circular capacitors with just 25  $\mu$ m-100  $\mu$ m diameter) resulted in small sub-picoampere response. To do this more accurately, localized thin-film heating would be required. As a result, researchers explored three complimentary approaches to locally heat and probe thin-film pyroelectric response across unprecedented frequency ranges [0.02 Hz to 1.3 MHz;<sup>33</sup> Fig. 3(a)]. One important approach introduced at this time, and subsequently utilized extensively, 11,22,35-37 made use of a microfabricated thin-film resistive heater patterned directly on top of the pyroelectric to oscillate its temperature [Fig. 3(b)] while simultaneously measuring pyroelectric currents [Fig. 3(c)]. 33,35 The

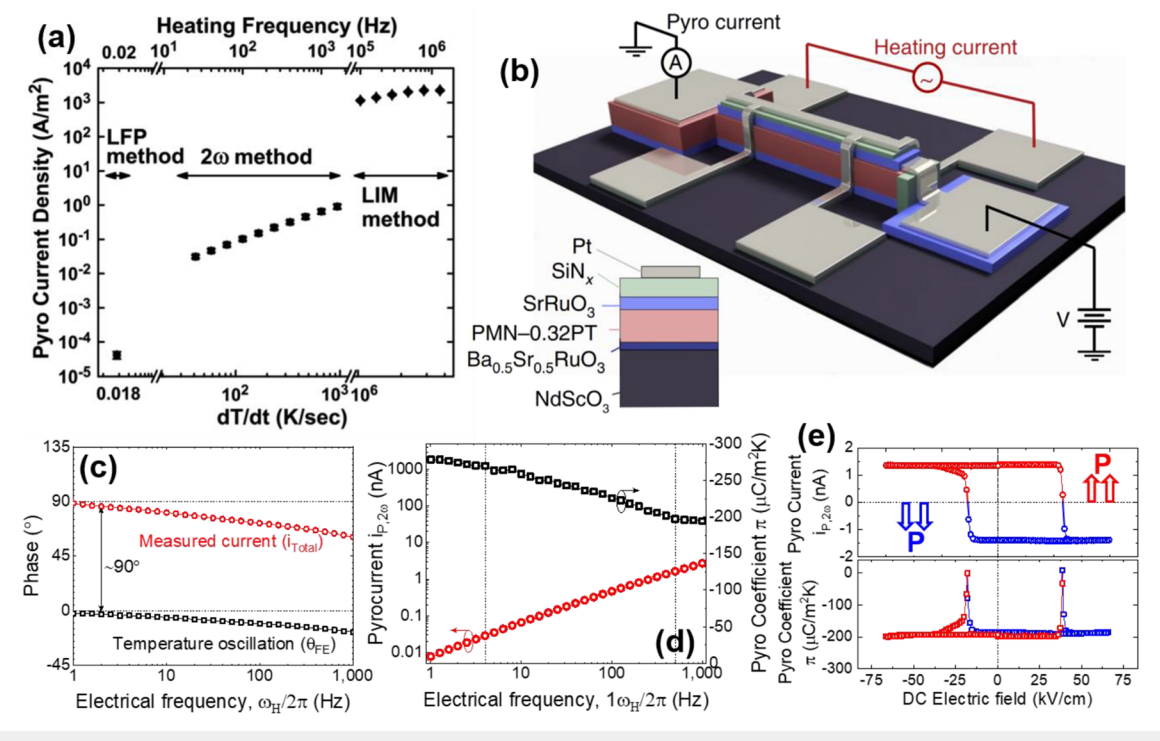


FIG. 3. (a) Pyroelectric current response across eight heating frequency decades only achievable in thin films using low frequency periodic (LFP),  $2\omega$ , and laser intensity modulation (LIM) characterization techniques.<sup>30</sup> (b) A nanofabricated thin film [100 nm 0.68Pb(Mg<sub>1/3</sub>Nb<sub>2/3</sub>)O<sub>3</sub>–0.32PbTiO<sub>3</sub> (PMN–0.32PT)] pyroelectric electrothermal test platform. With the utilization of thin film resistive heating and adapted 3-Omega temperature characterization methods, AC phase-sensitive pyroelectric measurements can effectively minimize spurious thermally stimulated current contributions to the total measured response.<sup>19</sup> Pyroelectric measurements of the PbZr<sub>0.2</sub>Ti<sub>0.8</sub>O<sub>3</sub> thin film including (c) the phase relationship of the measured current (at  $2\omega_H$ ) and the temperature oscillation (also at  $2\omega_H$ ) with respect to the phase of the applied heating current depicting that the measured current leads the temperature oscillation by ~90°. (d) Measured pyroelectric current and pyroelectric coefficient as a function of heating frequency. At low frequencies (<4 Hz),  $\pi \to \left(\frac{\partial P}{\partial T}\right)_{E,X}$ , while at high frequencies (>500 Hz),  $\pi \to \left(\frac{\partial P}{\partial T}\right)_{E,X}$  due to secondary contribution to pyroelectricity (reduction by ~30%). (e) Pyroelectric hysteresis loops as a function of the background DC electric field at 1 kHz.<sup>32</sup>

biggest advantage of this technique is that the applied temperature oscillation frequency was no longer limited to the sub-hertz regime but could be pushed out to the order of kilohertz, significantly enhancing the pyroelectric current  $(i_p \approx \frac{dT}{dt})$  [Fig. 3(d)]. Additionally, researchers developed another approach that utilized a modulated laser to locally heat the pyroelectric at frequencies up to the order of tens of megahertz.<sup>38</sup> Both of these AC techniques leverage advances from the thermal-sciences community (e.g., 3omega methods<sup>39</sup> and time-domain thermoreflectance<sup>40,41</sup>) as well as sophisticated nanoscale heat-transport modeling<sup>42</sup> to accurately predict the temperature change in the pyroelectric. Another advantage of these high-frequency techniques is their ability to separate out the secondary pyroelectric contribution from the primary contribution by controlling the thermal penetration depth using the frequency of the temperature oscillation, all the while controlling the background DC electric field [Fig. 3(e)]. In all, the localized high-frequency techniques enabled more accurate and more detailed characterization of pyroelectricity in thin films. Such techniques now provide scientists with some of the most advanced and accurate measurements of these effects and a way to quantify and differentiate various contributions to pyroelectricity.

#### IV. RECENT ADVANCES IN PYROELECTRIC THIN FILMS

### A. Models and simulations

The equilibrium properties of ferroelectrics and pyroelectrics in addition to their dependence on temperature, electric fields, and epitaxial stress/strain have generally been described by mean-field GLD thermodynamic models. There, the free energy of a ferroelectric is expanded as a power series of the order parameter (i.e., polarization) and then minimized to identify the properties at equilibrium. The effects of stress/strain, temperature, and electric fields are evaluated by adding appropriate coupling terms to the free energy. In the reference frame of the paraelectric phase, the free energy (F) may be written as  $^{44}$ 

$$F = \alpha_1 \left( P_1^2 + P_2^2 + P_3^2 \right) + \dots + \frac{1}{2} s_{11} \left( X_1^2 + X_2^2 + X_3^2 \right) - \dots + E_1 P_1$$
$$- E_2 P_2 - E_3 P_3,$$

where  $\alpha_i$  are the material dependent stiffness coefficients,  $P_i$  are the polarization components, and  $s_{ij}$  is the compliance tensor that describes the coupling between polarization and stress. The simplest such model assumes a monodomain polarization state and adequately captures the phenomenological features of pyroelectricity. Such approaches are, however, inadequate for thin films where epitaxial strain can induce complex domain structures, depolarization fields, thermal-expansion mismatch with the substrate, etc., all of which impact the equilibrium polarization. Recent work on phenomenological models has included increasing complexity, bringing such models closer to the realities of experiment and polycrystalline thin films where non-trivial domain structures exist.  $^{25,45-51}$  Such approaches have uncovered various effects that can impact pyroelectricity in thin films and allow for systematic optimization of pyroelectric figures of merit (FoMs).

These mean-field approaches, however, provide a purely macroscopic picture of the phenomena and do not predict the microscopic (atomistic) nature of the physics, thus limiting

suitability for non-equilibrium phenomena such as switching and leakage. These limitations of the equilibrium thermodynamic descriptions must be kept in mind as we use these approaches to understand and optimize thin-film materials. More broadly, this means that such formalisms are incapable of uncovering new pyroelectric materials and are further limited only to well-known material systems (e.g., BaTiO<sub>3</sub> and PbZr<sub>1-x</sub>Ti<sub>x</sub>O<sub>3</sub>), which have previously defined bulk descriptions. As a result, the development of first-principles/ab initio approaches to both understand the effects in materials and design new materials represents a clear need for investment by the community. What little work that does exist has only begun to scratch the surface of the connection between microscopic and macroscopic response in pyroelectrics and has not yet addressed these issues in the classical systems and geometries the broader community might desire.  $^{52,53}$ 

# **B.** Experimental studies

The past decade has seen numerous advances in experimental probes of pyroelectricity in thin films. Unlike bulk ceramics, thin films can maintain large strain states >±1% imposed by the underlying substrate and thus provide researchers considerable ability to manipulate and control polar order and domain structures. This is particularly interesting since all properties (i.e., dielectric, piezoelectric, and pyroelectric) can be strongly affected by changes in the transition temperatures, magnitude of polarization, and domain structures. The first work to probe such effects—namely, how ferroelectric domain structures impact property evolution—focused on PbZr<sub>0.2</sub>Ti<sub>0.8</sub>O<sub>3</sub> thin films where growth on different substrates (i.e., different lattice mismatches) produced domain structures with varying fractions of out-of-plane oriented c domains and in-plane oriented a domains. In turn, researchers combined both GLD approaches and experimental studies to directly quantify the extrinsic contribution of both dielectric 10 and pyroelectric<sup>9</sup> response [Fig. 4(a)]. This represented the first attempt to establish and directly measure an analogous extrinsic contribution to pyroelectricity and concurrently demonstrated that secondary contribution arising from the thermal-expansion mismatch of the film and substrate could be substantial (accounting for 25%-50% of the response). Subsequent work has built from these early studies, leveraging more advanced measurement techniques, to further quantify extrinsic contributions to pyroelectricity. For example, again using PbZr<sub>0.2</sub>Ti<sub>0.8</sub>O<sub>3</sub> as a model system, researchers used a range of substrates and strain states together with temperature-dependent scanning-probe microscopy and x-ray diffraction to observe similar trends.<sup>37</sup> Here, by referencing a purely c-oriented monodomain film and adjusting for the strain-induced variation of polarization, researchers were able to quantify both the intrinsic and extrinsic effects, showing that the latter could be as much as 35% of the total measured pyroelectric response and that the strain state (compressive strains diminished and tensile strains enhanced) affects the temperature-driven domain interconversion and thus the overall pyroelectric response [Fig. 4(b)].

In turn, researchers undertook further studies aimed at illuminating the various contributions to pyroelectric response. Specifically, work combining both GLD models and experiments focused on  $PbZr_{0.52}Ti_{0.48}O_3$  (perched at the morphotropic phase boundary) films was also able to directly quantify the magnitude and

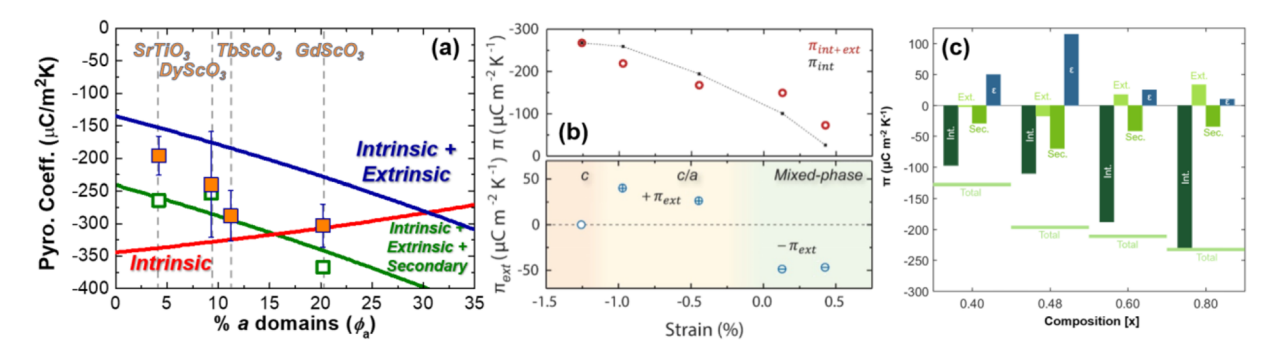


**FIG. 4.** (a) The measured pyroelectric coefficient (filled orange squares) as a function of a domain percentage in polydomain PbZr<sub>0.2</sub>Ti<sub>0.8</sub>O<sub>3</sub> thin films. The red line is the intrinsic response, while the blue line depicts the primary response (intrinsic + extrinsic) calculated using polydomain GLD theory. The open green squares indicate the sum of primary + secondary contributions to the pyroelectric coefficient for each film–substrate combination and the green line indicates the trend expected assuming an average thermal expansion coefficient of  $10.9 \times 10^{-6}$  K<sup>-1</sup> for all the substrates.<sup>9</sup> (b) First reported experimental quantification of extrinsic domain-wall contributions to pyroelectricity. Through the systematic control of mechanical strain, the ferroelastic domain structure may be tuned in thin film pyroelectrics to elucidate not only the magnitude of extrinsic contributions but also the sign (i.e., >0 or <0).<sup>34</sup> (c) Summary of the intrinsic, extrinsic, secondary, and total pyroelectric response as a function of the composition across the various PbZr<sub>1-x</sub>Ti<sub>x</sub>O<sub>3</sub> chemistries. Due to the opposing signs of the various contributions, the total net pyroelectric coefficient value is indicated via a solid line for each composition. The dielectric contribution displayed here is that measured at an applied dc-electric field of 100 kV cm<sup>-1</sup>.

direction of the secondary and field-induced pyroelectric effects.<sup>54</sup> In a similar spirit, recent work has quantified the intrinsic, extrinsic, dielectric, and secondary pyroelectric contributions for the  $PbZr_{1-x}Ti_xO_3$  (x = 0.40, 0.48, 0.60, and 0.80) system without the need for a monodomain reference material.<sup>11</sup> Using a combination of direct high frequency and high applied DC voltage measurements, researchers managed to systematically suppress and individually quantify all contributions [Fig. 4(c)]. It was found that the DC voltage could be used to suppress both the dielectric and extrinsic contributions, while high frequency heating allowed for the suppression of secondary contributions. Not only was the intrinsic pyroelectric response measured this way, but the researchers also explored the evolution of both the magnitude and the sign of the dielectric and extrinsic contributions across the morphotropic phase boundary of the PbZr<sub>1-x</sub>Ti<sub>x</sub>O<sub>3</sub> system. Similar observations have recently been seen in Pb<sub>0.99</sub>[(Zr<sub>0.52</sub>Ti<sub>0.48</sub>)<sub>0.98</sub>Nb<sub>0.02</sub>]O<sub>3</sub> thin films on both nickel foils and silicon wafers where dramatic differences in room temperature pyroelectric response were measured due to differences in the various pyroelectric contributions on these substrates.<sup>55</sup> In all, such reports of pyroelectric contribution extraction have elucidated the difference in susceptibility enhancement design rules between pyroelectrics and their dielectric/piezoelectric counterparts.

# C. New thin-film pyroelectric materials

The advent of new and better measurement approaches has opened the potential for researchers to explore new systems. For example, researchers have probed compositionally graded ferroelectrics in which the chemistry of the material is varied across the thickness of the film. Recent studies of epitaxially grown compositionally graded films revealed the potential for exotic domain structures and properties,  $^{23,56,57}$  which were further extended to pyroelectricity. Focusing on compositionally graded films transitioning from  $PbZr_{0.2}Ti_{0.8}O_3$  to  $PbZr_{0.8}Ti_{0.2}O_3$  and vice versa, researchers were able to independently control the pyroelectric coefficient [Fig. 5(a)]

and the dielectric permittivity to increase the material performance and FoMs for various applications [Fig. 5(b), see details in Sec. V A].  $^{58}$  The compositional gradients result in large strain gradients ( $\sim 10^5 \, \mathrm{m}^{-1}$  to  $10^6 \, \mathrm{m}^{-1}$ ; not achievable in bulk), which, in turn, generate large built-in potentials that can reduce the permittivity while maintaining large pyroelectric response. In the end, the work showed a route to enhance the pyroelectric FoMs of materials by 3-12 times in comparison to standard materials.

Recent work has also explored pyroelectricity in some of the most complex ferroic materials in the community, the so-called relaxor ferroelectrics. These materials exhibit a characteristic broad dielectric response with temperature and strong dielectric relaxation with frequency, which are generally attributed to the formation of polar nano-regions/domains. Leveraging advances in thinfilm synthesis of these materials<sup>59,60</sup> and building from the already robust performance demonstrated in micrometer-thick pyroelectric ceramic relaxor ferroelectrics, 61 new studies have exploited strong field- and temperature-induced polarization susceptibilities in 0.68Pb(Mg<sub>1/3</sub>Nb<sub>2/3</sub>)O<sub>3</sub>-0.32PbTiO<sub>3</sub> to produce record-breaking PEC (see Sec. V A).<sup>22</sup> Electric-field-driven enhancement of the pyroelectric response [which was measured to be as large as -550  $\mu$ C m<sup>-2</sup> K<sup>-1</sup>, Fig. 5(c)] and suppression of the dielectric response (by up to 72%) yielded substantial FoMs for PEC [Fig. 5(d)]. Field- and temperature-dependent pyroelectric measurements highlighted the role of polarization rotation and field-induced polarization in mediating these effects. This opens a new class of materials that could have increasingly interesting effects, especially under field-driven conditions for pyroelectric applications.

Finally, recent years have seen a dramatic investment in the study of novel ferroelectric materials such as the hafnia-based systems, including the work to probe pyroelectricity. Early efforts  $^{62}$  using indirect measurements claimed (surprisingly) large pyroelectric effects in silicon-doped HfO<sub>2</sub>, which was attributed to a temperature-driven phase transition. This work, however, came into question when researchers applied phase-sensitive detection approaches on zirconium- $^{63}$  and silicon-doped HfO<sub>2</sub>, $^{64,65}$  which

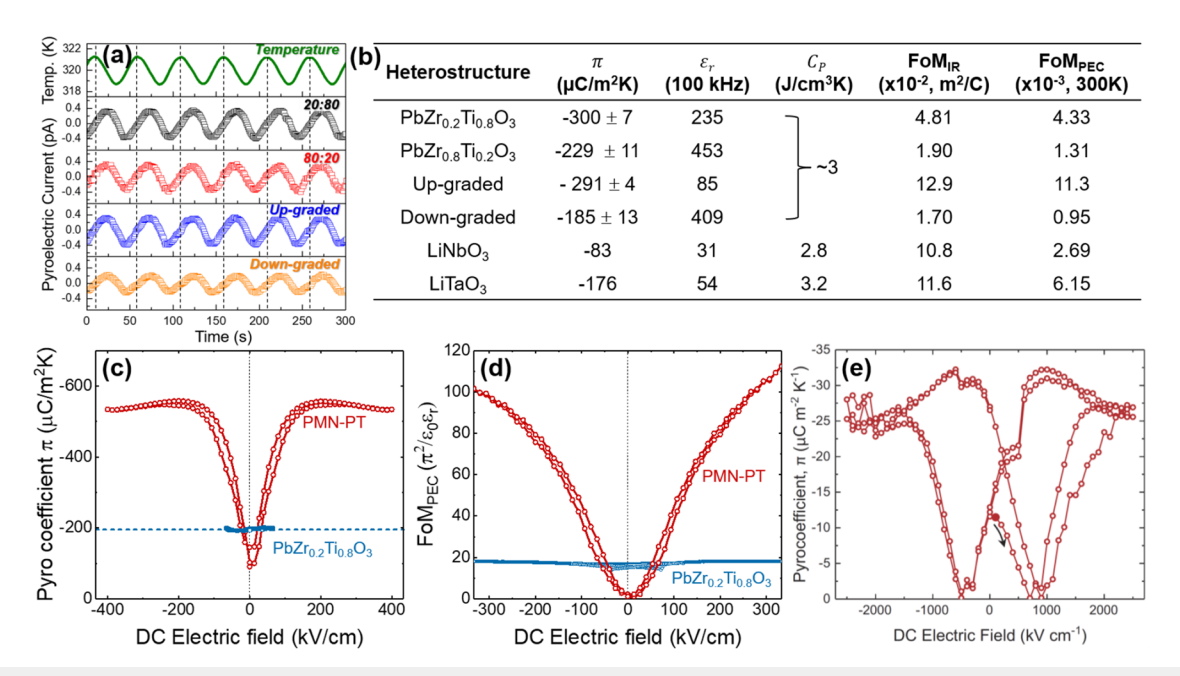


FIG. 5. (a) Top to bottom: sinusoidal temperature variation applied to extract pyroelectric responses of single-layer PbZr<sub>0.2</sub>Ti<sub>0.8</sub>O<sub>3</sub> (20:80), single-layer PbZr<sub>0.8</sub>Ti<sub>0.2</sub>O<sub>3</sub> (80:20), and compositionally up-graded and compositionally down-graded heterostructures. (b) Table summarizing the pyroelectric coefficients ( $\pi$ ), dielectric permittivity ( $\epsilon_r$ ), heat capacity ( $C_p$ ), thermal imaging figure of merit (FoM<sub>IR</sub>), and pyroelectric energy conversion figure of merit (FoM<sub>PEC</sub>) for compositionally graded and non-graded pyroelectric materials. (c) Pyroelectric coefficient and (d) FoM<sub>PEC</sub> as a function of the dc electric field for a 0.68PbMg<sub>1/3</sub>Nb<sub>2/3</sub>O<sub>3</sub>-0.32PbTiO<sub>3</sub> (PMN-PT) and a PbZr<sub>0.2</sub>Ti<sub>0.8</sub>O<sub>3</sub> thin film measured in the same configuration. (e) Pyroelectric coefficient measured as a function of the background dc electric field at 1 kHz for a silicon-doped HfO<sub>2</sub> thin film. The black arrow and red filled data point show the direction and starting point of the measurements. (a)

suggested that the effects are rather modest. Using an advanced microfabricated pyroelectric measurement setup, researchers were able to undertake a comprehensive zero-field and field-dependent study of pyroelectricity to show that thin films of silicon-doped HfO2 exhibit pyroelectric response with a "wake-up" behavior akin to the wake-up phenomenon observed in the ferroelectric polarization with electric-field cycling. This pyroelectric response was found to be rather small ( $\sim 25 \ \mu \text{C m}^{-2} \ \text{K}^{-1}$ ), which was consistent with other phase-sensitive measurements [Fig. 5(e)]. Surprisingly, however, simultaneous direct electrocaloric measurements revealed an electrocaloric coefficient ~4 times larger in magnitude than that expected for the measured pyroelectric coefficient. This enhancement was explained using the plausible role played by defect dipoles that not only contributed to additional configurational or dipolar entropy but also dictated the wake-up behavior in polarization and pyroelectricity.3

#### V. APPLICATIONS OF PYROELECTRIC THIN FILMS

# A. Figures of merit for pyroelectric applications

Since the 1960s, pyroelectrics have found their way into various thermal imaging, thermal sensing, and gas monitoring applications, owing mostly to their intrinsic insensitivity to a wide wavelength spectrum, speed, and room-temperature performance. <sup>15,66,67</sup> The relative potential of a material for a given application can be described by an appropriate FoM. For pyroelectrics, these include (1) thermal (infrared) sensors and electron emitters where the FoM

is  $\pi/C_p \varepsilon_0 \varepsilon_r$  and  $C_p$  is the specific heat capacity<sup>15,68</sup> and (2) PEC where the FoM is  $\pi^2/\varepsilon_0\varepsilon_r$  or the closely related electrothermal coupling coefficient  $k^2 = \pi^2 T/C_p \varepsilon_0 \varepsilon_r$ , where T is the temperature of operation. 69-71 Such FoMs provide a simple but informative description of the tradeoffs at play in typical applications and provide material scientists guidance on how to control materials in useful ways to improve the overall performance. From these FoMs, the design challenges for pyroelectric materials are clear—produce a large pyroelectric coefficient, a small heat capacity, and a small dielectric permittivity for all applications. Many of the highest performance pyroelectric materials are complex oxide systems with generic ABO3 chemistry, which generally possess heat capacity values that lie within a relatively small range (2 J/cm<sup>3</sup> K-3.2 J/cm<sup>3</sup> K), <sup>17,70</sup> making it an ineffective tuning parameter. This leaves independently enhancing the pyroelectric coefficient and suppressing the dielectric permittivity; an optimization process that is difficult in conventional materials where dielectric and pyroelectric responses are generally enhanced by the same generic features. Some approaches (see Sec. IV C) have been successful in addressing this design tradeoff. Here, we highlight two areas where recent work on thin films has made impact.

# B. Pyroelectric energy conversion

The need for PEC is clear—nearly two-thirds of the primary energy produced in the U.S. is lost as waste heat; a significant portion of which is considered as low-grade (i.e., 100°C-230°C).

Unlike thermoelectrics that utilize a spatial-temperature gradient, PEC requires a temporal variation in temperature  $(\partial T/\partial t)$ , making PEC highly desirable in instances where temperature gradients are either difficult to establish or the temperature of the heat source is fluctuating. These temperature changes result in a pyroelectric current  $i_p = \pi A \left( \frac{\partial T}{\partial t} \right)$ , which equates to performance scaling with the area, not the volume. This leads to a number of potential advantages for thin-film devices and thus motivates the focus on materials in such geometries here. To harvest waste heat, a PEC device mimics a thermodynamic heat engine leveraging a variety of cycles<sup>73,74</sup> distinguished by their polarization vs electric-field pathways [Figs. 6(a)-6(e)]. The power density is governed by the combined electrical and thermal-time constant of the device and thus scales with the frequency of temperature oscillation. Often, the thermal-time constant can be much larger than the electrical-time constant and is, therefore, the limiting factor in achieving a large power density. It has been shown<sup>22</sup> that thin-film devices inherently have a better power density than bulk devices.<sup>75</sup> For example, in thin-film relaxors, researchers have achieved a power density that is three orders of magnitude larger than that of bulk versions, despite having an energy density that is only one order of magnitude larger. It should be noted that the trend in thin-film research is to calculate the energy and power densities for the volume of the thin film only (excluding the substrate) in an attempt to allow for direct comparison to bulk materials. Regardless, looking forward, it appears that

thin-film geometries are promising for future pyroelectric device design.

### C. Electron emission

For a detailed description and review of pyroelectric (thermally driven) electron emission, see Ref. 5. Here, we briefly provide a recap of the field and the efforts within thin films. Defined via the opencircuit configuration  $V = \frac{\pi}{\varepsilon_{33}^{\sigma}} d\Delta T$ , where d and  $\varepsilon_{33}^{\sigma}$  refer to thickness and dielectric permittivity at constant stress, respectively, pyroelectric emission is a special case of field emission, where the energy necessary for electrons to tunnel into vacuum is provided by internally bound charges rather than an external electric field. Provided a rapid enough temperature change, a pyroelectric material can generate a large field (typically  $10^2 \text{ V/}\mu\text{m}-10^4 \text{ V/}\mu\text{m}^{5,68,76}$ ), which can eject electrons into vacuum. Rather than depending on the absolute temperature of the system, pyroelectric electron emission is uniquely determined by the rate of change of temperature when operated below the phase-transition temperature.<sup>77-80</sup> Compared to thermionic or field emitters, pyroelectric emitters can operate with a temperature variation of only a few degrees, emit high-energy electrons with no acceleration, and produce large current densities. Most work, however, has focused on pyroelectric materials with thicknesses  $>50 \mu m$ , thus limiting their integration into modern microelectronics. To

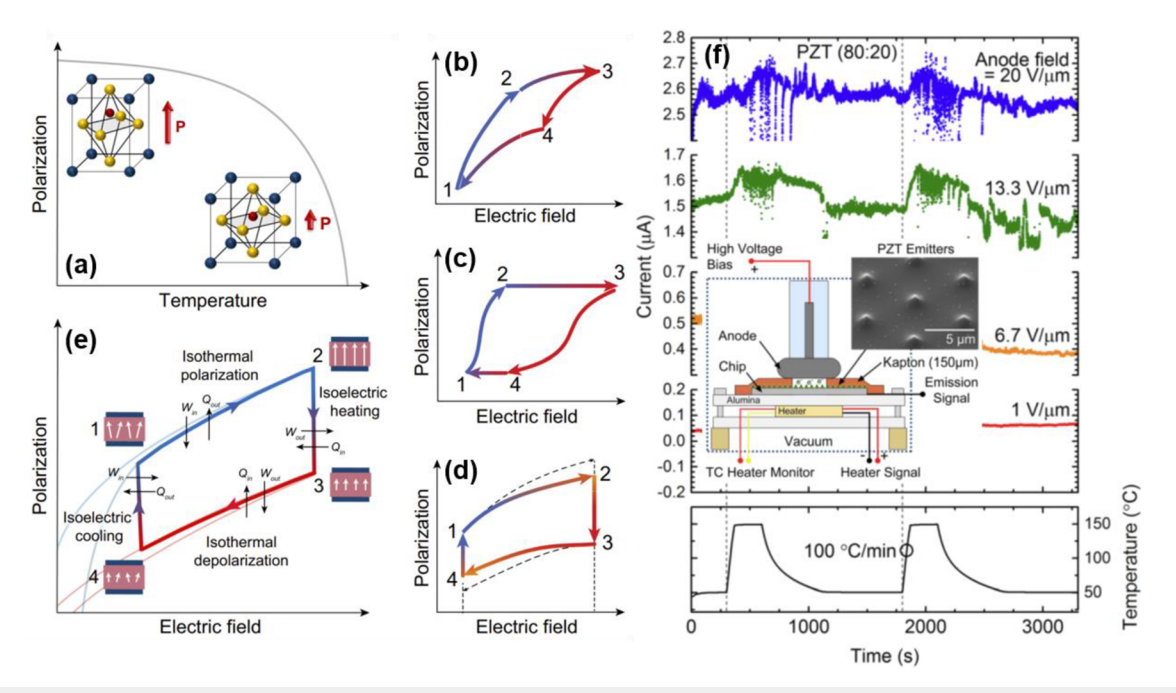


**FIG. 6.** (a) Depiction of the temperature dependence of the spontaneous polarization (P) and associated electrical dipole displacements at the unit cell level of the perovskite structure. (b) Carnot, (c) Stirling, (d) Brayton, and (e) Ericsson (Olsen) cycles use for pyroelectric waste-heat energy conversion. (f) Pyroelectric emission from a PbZr<sub>0.8</sub>Ti<sub>0.2</sub>O<sub>3</sub> thin film with varying electric field strengths. The noise arises from surface flashover events and discharge from the anode to the pyroemitters (bottom) The sample was actively heated at 100 °C/min but passively cooled for two cycles. Inset: experimental setup for pyroelectric electron emission. Tip emitter samples are tested in a vacuum chamber at 10<sup>-6</sup> Torr to 10<sup>-7</sup> Torr. The samples were secured to an alumina plate using silver paint and separated from the anode using a Kapton tape of 150  $\mu$ m thick. A ceramic heater heated the samples from the bottom, while the anode generated a macroscopic electric field using a positive voltage bias. A SEM micrograph of a microfabricated tip emitter array coated with a 30-nm-thick epitaxial pyroelectric film. The tips have a mean tip radius of

achieve pyroelectric emission from films in the 20 nm–20 000 nm thickness range, heating rates of up to  $10^9\,^{\circ}$  C/min are required to overcome other electric compensation mechanisms (e.g., leakage). Recent attempts to miniaturize these effects have focused on integrating thin films of pyroelectrics with microelectromechanical systems (MEMS) where it is possible to produce such heating rates. For example, researchers were able to directly synthesize 30-nm-thick films of PbZr<sub>x</sub>Ti<sub>1-x</sub>O<sub>3</sub> (of various compositions) on arrays of silicon nanoemitters and achieve both field and thermal emission [Fig. 6(f)]. In the latter, the emitted charge was 7% of that expected for a perfect thin film, and the pyroelectric emission was calculated to occur without an applied field if the heating rate exceeded  $4\times10^7\,^{\circ}$ C/min.

# VI. LOOKING TO THE FUTURE-PYROELECTRICITY AND BEYOND

# A. Large and novel pyroelectric effects and FoMs

While we know how to produce large pyroelectric response (e.g., by perching a material near a chemically or structurally induced phase boundary), such routes are, in general, highly temperature dependent and shown to simultaneously enhance dielectric permittivity, which drives down FoMs. While initial studies are promising in addressing some of these concerns, there is considerable work to be done. A number of important questions remain: Can we make new materials (or even new versions of known materials) with record-breaking pyroelectric coefficients? Can we develop additional routes to increase pyroelectric currents while suppressing the dielectric permittivity? The community has not applied the same diligence and dedication given to the design of dielectric, piezoelectric, ferroelectric, or multiferroic materials. One can image design approaches working not only at the ab initio and unit-cell levels in identifying materials with exotic temperature dependence for their polar order but also at the mesoscale level identifying materials with designer domain structures that produce larger than expected composite pyroelectric effects. The design space is immense and requires specific approaches to address the dearth of high-performance materials. The values of pyroelectricity (away from a phase transition) for most materials studied to date lie within about one order of magnitude of each other-begging the question of how larger effects near room temperature can be achieved?

# B. Novel pyroelectric phenomena from emergent topologies

Progress in the synthesis of nearly perfect oxide interfaces with unit-cell control has allowed the creation of superlattice heterostructures where emergent phenomena such as new polar topologies (skyrmions and vortex structures)<sup>83,84</sup> are characterized by an additional order parameter: the electric toroidal moment. The toroidal moment, originally proposed for zero-dimensional ferroelectrics,<sup>85</sup> should give rise to new phases (ferrotoroidic and antiferrotoroidic), as well as new electromechanical (piezotoroidic) and electrothermal (pyrotoroidic) couplings. The latter emerges from the temperature dependence of the toroidal moment described by the corresponding pyrotoroidic tensor.<sup>86</sup> The converse effect, the toroidocaloric effect,<sup>87</sup> is also possible, where a curl of the electric field produces

a temperature change in a system with polar vortices. Today, we await a careful study of these effects.

# C. Pyromagnetism and pyro-electric-magnetic effects

The pyromagnetic effect is analogous to the pyroelectric effect—it is the change in the spontaneous magnetization of a material with a change in temperature (Chynoweth also developed a dynamic method to measure this effect).<sup>88</sup> The question then arises: Can we use the pyromagnetic and pyroelectric effects in tandem to achieve something new? Leveraging advances in materials, pyroelectric measurements, and related fields such as multiferroics and magnetoelectrics, the community seems poised to address this question. What one might call pyro-electric-magnetic effects could be possible in multiferroic/magnetoelectric systems wherein one obtains both pyroelectric (from the polar order) and pyromagnetic (from the magnetic order) effects from a single or composite system. This could, in turn, produce larger values of pyroelectric current, provide for new coupling effects, or open the way for novel applications. For example, the field of thermomagnetic conversion has been studied for some years<sup>89</sup> and is, again, analogous to PEC. The idea is that temperature oscillations drive a time-varying magnetic flux that induces a current in a solenoid. Could a composite structure be designed that leverages these two effects (pyroelectric energy and thermomagnetic conversion) to create new record-breaking conversion efficiencies and energy/power densities?

# D. Electrocaloric effects: Leveraging new measurement platforms

The measurement protocols developed in the past few years for pyroelectrics can also be applied to other effects, such as the electrocaloric effect. The small thermal mass of thin films with respect to the supporting substrates has so far prevented the direct measurement of these temperature changes, which are (like pyroelectricity) primarily obtained indirectly by measuring the temperature dependence of the order parameter and applying Maxwell relations to obtain temperature and entropy changes. In order to be applied correctly, these relations require knowledge of the temperature and field dependence of heat capacity and careful attention to the boundary conditions (i.e., the stress/strain state of the film) in order to obtain accurate results. The novel electrothermal test devices developed for the accurate measurement of pyroelectric current also provide new direct probe capabilities for electrocaloric temperature changes. Indeed, researchers have<sup>35</sup> registered temperature changes as small as millikelvins for a 150-nm-thick ferroelectric thin film in response to an electric field. Further measurements near phase transitions are required in order to verify the giant electrocaloric response reported for thin films via indirect methods. Other techniques such as infrared lock-in thermography<sup>90</sup> may also enable non-contact and spatially resolved studies of caloric responses, provided that the heat transfer to the substrate can be reduced by fabricating suspended ferroelectric membranes. 91,92 Such "mechanically free" membranes could also enable the study of piezocaloric<sup>93</sup> (polarization-dependent), elastocaloric<sup>94</sup> (strain-dependent), and flexocaloric<sup>95</sup> (strain gradient-dependent) effects where strain is no longer dominated by underlying substrates, but by the elastic compliance, thickness, and lattice misfit of the various constituent material layers of the heterostructure<sup>96</sup>

Such approaches could also allow for unprecedented function of pyroelectric-based thermal imaging/sensing devices—the full implications of these observations, however, remains to be seen as more work is undertaken.

### E. Ferroelectric thermoelectrics

In comparison to pyroelectric, thermomagnetic, and thermoelastic energy conversion, thermoelectrics have received wider attention. Several strategies exploiting the physics of ferroelectrics for thermoelectric applications have been proposed. Se-100 For example, the coupling of soft-polar phonons associated with ferroelectric instabilities with heat carrying acoustic phonons was shown to induce scattering, effectively reducing the lattice thermal conductivity in tellurides without suppressing electrical transport. Conductivity in tellurides without suppressing electrical transport. Conductivity in addition to increased interfacial thermal resistance (Kapitza resistance) with respect to the typical values obtained in grain boundaries. Moreover, the ability to manipulate the domains with electric fields enables the electrical manipulation of thermal transport, Conductivity in microelectronic devices.

# F. Pyroelectric devices of tomorrow

Building from this work, we are beginning to see new ideas of how these materials will be used in the coming years. For example, within the realm of PEC, one of the challenges has been to envision how one generates the required time-varying temperature profile. One approach focused on the use of a modulated laser heat source that provides both high frequency thermal cycles and long-distance energy transfer.<sup>107</sup> Key to this work was developing a low-reflectivity nanostructured IrO2 top electrode to absorb the incident radiation. In other work, researchers showed the potential for a portable power concept using PEC driven by the heat from on-chip catalytic combustion of methanol. This ingenious approach takes advantage of the high energy density of liquid fuels (22 MJ/kg for methanol) and the ability to directly apply and combust such fuels to demonstrate a pathway to energy densities comparable to lithium-ion batteries (~0.8 MJ/kg).<sup>108</sup> Other available routes to impact the needs of PEC include addressing the fact that nearly all pyroelectric materials have high specific heats. Identification of new classes of materials with lower specific heat but similar pyroelectric performance would result in more effective utilization of heat sources. Additionally, new efforts focused on regenerative schemes employing multi-staged heat reservoirs have also been proposed to reduce the total heat input and thus increase the efficiency. 109 At the same time, there is a push to develop new energy-harvesting cycles to maximize performance, including considering hybrid cycles. In this spirit, combined piezo/pyroelectric devices have demonstrated larger maximum output voltages<sup>110-112</sup> and stretchable hybrid energy-scavenging nanogenerators based on polymer systems<sup>113</sup> and others have even fabricated thin films capable of harvesting solar, thermal, and mechanical energies. 114 Additionally, combined ferro-/antiferroelectric cycles have been realized in a single device, taking advantage of the bidirectional nature of the pyroelectric coefficient in these materials. 115 These hybrid generators aim to increase the device performance by integrating systems to maximize the extractable energy between two temperature extrema.

Pyroelectrics have substantially progressed in recent years. While compared to dielectric, piezoelectric, and even electrocaloric effects, pyroelectricity has received less attention, the potential for pyroelectrics to make impact on modern applications is as real as any in these areas. Continued attention to understanding the fundamental nature of these materials and their physical mechanisms while simultaneously developing ways to utilize them in real applications is needed. Pyroelectrics have, over the past few decades, already played a key role in a range of applications we use on a daily basis and, looking to the future, the advent of advanced thin-film pyroelectrics stands poised to open up a new generation of applications.

#### **ACKNOWLEDGMENTS**

We write this review on behalf of numerous collaborators and colleagues who have provided critical insights, support, and feedback. In particular, we acknowledge the support of Professor David Cahill and Professor William King and their respective groups at the University of Illinois, Urbana-Champaign, as well as Professor Chris Dames and his group at the University of California, Berkeley, for their contributions to the development and implementation of novel pyroelectric measurements and devices based on thin-film materials. Over the years, our team received support from numerous sources for the development of these techniques and scientific studies, including the Air Force Office of Scientific Research (Grant No. AF FA 9550-11-1-0073), the Army Research Office (Grant Nos. W911NF-10-1-0482 and W911NF-14-1-0104), the Office of Naval Research (Grant No. N00014-10-1-0525), the National Science Foundation (Grant Nos. DMR-1149062, DMR-1451219, and DMR-1708615), the European Union's Horizon 2020 (Marie Skłodowska-Curie Grant No. 797123), and the U.S. Department of Energy, Office of Basic Energy Sciences [Grant Nos. DEFG02-07ER46459 and DE-AC02-05-CH11231 (Materials Project Program No. KC23MP)].

# **DATA AVAILABILITY**

Data sharing is not applicable to this article as no new data were created or analyzed in this study.

#### **REFERENCES**

- <sup>1</sup>E. R. Caley and J. F. C. Richards, *Theophrastus on Stones* (The Ohio State University, Columbus, 1956).
- <sup>2</sup>M. E. Lines and A. M. Glass, *Principles and Applications of Ferroelectrics and Related Materials* (Oxford University Press, New York, 1977).
- <sup>3</sup>R. W. Whatmore and R. Watton, Ferroelectrics 236, 259–279 (2000).
- <sup>4</sup>S. P. Alpay, J. Mantese, S. Trolier-McKinstry, Q. Zhang, and R. W. Whatmore, MRS Bull. **39**, 1099–1111 (2014).
- <sup>5</sup>G. Rosenman, D. Shur, Y. E. Krasik, and A. Dunaevsky, J. Appl. Phys. 88, 6109–6161 (2000).
- <sup>6</sup>E. Fatuzzo and W. J. Merz, *Ferroelectricity* (North Holland, Amsterdam, 1967).
- <sup>7</sup>L. W. Martin and A. M. Rappe, Nat. Rev. Mater. 2, 16087 (2017).
- <sup>8</sup> J. Karthik and L. W. Martin, Phys. Rev. B **84**, 024102 (2011).
- <sup>9</sup>J. Karthik, J. C. Agar, A. R. Damodaran, and L. W. Martin, Phys. Rev. Lett. 109, 257602 (2012).
- <sup>10</sup>J. Karthik, A. R. Damodaran, and L. W. Martin, Phys. Rev. Lett. **108**, 167601 (2012).
- <sup>11</sup>G. Velarde, S. Pandya, L. Zhang, D. Garcia, E. Lupi, R. Gao, J. D. Wilbur, C. Dames, and L. W. Martin, ACS Appl. Mater. Interfaces 11, 35146–35154 (2019).

- <sup>12</sup>Y. Tang, S. Zhang, Z. Shen, W. Jiang, J. Luo, R. Sahul, and T. R. Shrout, J. Appl. Phys. 114, 084105 (2013).
- <sup>13</sup> J. D. Zook and S. T. Liu, J. Appl. Phys. **49**, 4604–4606 (1978).
- <sup>14</sup>V. F. Kosorotov, L. S. Kremenchugskij, L. V. Levash, and L. V. Shchedrina, Ferroelectrics 70, 27–37 (1986).
- <sup>15</sup>R. W. Whatmore, Rep. Prog. Phys. 49, 1335-1386 (1986).
- <sup>16</sup>S. B. Lang, Sourcebook of Pyroelectricity (CRC Press, 1974).
- <sup>17</sup>P. Muralt, Rep. Prog. Phys. **64**, 1339–1388 (2001).
- <sup>18</sup> M. Kohli, A. Seifert, B. Willing, K. Brooks, and P. Muralt, Integr. Ferroelectr. 17, 359–367 (1997).
- <sup>19</sup>C. M. Hanson, H. R. Beratan, R. A. Owen, M. Corbin, and S. McKenney, Proc. SPIE **1735**, 17 (1992).
- <sup>20</sup> R. A. Owen, J. F. Belcher, H. R. Beratan, and S. N. Frank, Proc. SPIE 2746, 101 (1996).
- <sup>21</sup> J. F. Belcher, C. M. Hanson, H. R. Beratan, K. R. Udayakumar, and K. L. Soch, SPIE 3436, 611 (1998).
- <sup>22</sup>S. Pandya, J. Wilbur, J. Kim, R. Gao, A. Dasgupta, C. Dames, and L. W. Martin, Nat. Mater. 17, 432–438 (2018).
- <sup>23</sup> A. R. Damodaran, S. Pandya, Y. Qi, S.-L. Hsu, C. Nelson, A. Dasgupta, P. Ercius, C. Ophus, L. R. Dedon, J. C. Agar, H. Lu, J. Zhang, A. M. Minor, A. M. Rappe, and L. W. Martin, Nat. Commun. 8, 14961 (2017).
- <sup>24</sup> H. Zhao, W. Ren, and X. Liu, Ceram. Int. 43, S464–S469 (2017).
- <sup>25</sup> A. Sharma, Z.-G. Ban, S. P. Alpay, and J. V.Mantese, J. Appl. Phys. 95, 3618–3625 (2004).
- <sup>26</sup>S. Jachalke, E. Mehner, H. Stöcker, J. Hanzig, M. Sonntag, T. Weigel, T. Leisegang, and D. C. Meyer, Appl. Phys. Rev. 4, 021303 (2017).
- <sup>27</sup>D. W. Denlinger, E. N. Abarra, K. Allen, P. W. Rooney, M. T. Messer, S. K. Watson, and F. Hellman, Rev. Sci. Instrum. 65, 946–959 (1994).
- <sup>28</sup> A. G. Chynoweth, J. Appl. Phys. **27**, 78–84 (1956).
- <sup>29</sup> R. L. Byer and C. B. Roundy, Ferroelectrics **3**, 333–338 (1972).
- <sup>30</sup>L. E. Garn and E. J. Sharp, J. Appl. Phys. **53**, 8974–8979 (1982).
- <sup>31</sup> L. Pintilie, M. Alexe, I. Pintilie, and I. Boierasu, Ferroelectrics **201**, 217 (1997).
- <sup>32</sup> H. Okino, Y. Toyoda, M. Shimizu, T. Horiuchi, T. Shiosaki, and K. Matsushige, Jpn. J. Appl. Phys., Part 1 37, 5137 (1998).
- <sup>33</sup>B. Bhatia, J. Karthik, T. Tong, D. G. Cahill, L. W. Martin, and W. P. King, J. Appl. Phys. **112**, 104106 (2012).
- <sup>34</sup> L. Zhang, Y.-L. Huang, G. Velarde, A. Ghosh, S. Pandya, D. Garcia, R. Ramesh, and L. W. Martin, APL Mater. 7, 111111 (2019).
- 35 S. Pandya, J. D. Wilbur, B. Bhatia, A. R. Damodaran, C. Monachon, A. Dasgupta, W. P. King, C. Dames, and L. W. Martin, Phys. Rev. Appl. 7, 034025 (2017).
- <sup>36</sup>S. Pandya, G. Velarde, L. Zhang, and L. W. Martin, Phys. Rev. Mater. 2, 124405 (2018).
- <sup>37</sup>S. Pandya, G. A. Velarde, R. Gao, A. S. Everhardt, J. D. Wilbur, R. Xu, J. T. Maher, J. C. Agar, C. Dames, and L. W. Martin, Adv. Mater. 31, 1803312 (2019).
- <sup>38</sup>T. Tong, J. Karthik, L. W. Martin, and D. G. Cahill, *Phys. Rev. B* **90**, 155423 (2014).
- <sup>39</sup>D. G. Cahill, Rev. Sci. Instrum. **61**, 802–808 (1990).
- <sup>40</sup>D. G. Cahill, Rev. Sci. Instrum. 75, 5119 (2004).
- <sup>41</sup> A. J. Schmidt, X. Chen, and G. Chen, Rev. Sci. Instrum. **79**, 114902 (2008).
- <sup>42</sup>D. G. Cahill, W. K. Ford, K. E. Goodson, G. D. Mahan, A. Majumdar, H. J. Maris, R. Merlin, and S. R. Phillpot, J. Appl. Phys. 93, 793–818 (2003).
- <sup>43</sup> J. Zhang, J. C. Agar, and L. W. Martin, J. Appl. Phys. 118, 244101 (2015).
- <sup>44</sup>J. Karthik and L. W. Martin, Appl. Phys. Lett. **99**, 032904 (2011).
- <sup>45</sup> A. N. Morozovska, E. A. Eliseev, M. D. Glinchuk, L. Q. Chen, S. V. Kalinin, and V. Gopalan, Ferroelectrics 438, 32–44 (2012).
- <sup>46</sup> A. N. Morozovska, E. A. Eliseev, S. V. Kalinin, L. Q. Chen, and V. Gopalan, Appl. Phys. Lett. **100**, 142902 (2012).
- <sup>47</sup>A. N. Morozovska, E. A. Eliseev, S. L. Bravina, A. Y. Borisevich, and S. V. Kalinin, J. Appl. Phys. **112**, 064111 (2012).
- <sup>48</sup> J. Zhang, M. W. Cole, and S. P. Alpay, J. Appl. Phys. **108**, 054103 (2010).
- <sup>49</sup>M. T. Kesim, J. Zhang, S. P. Alpay, and L. W. Martin, Appl. Phys. Lett. 105, 052901 (2014).

- <sup>50</sup> M. T. Kesim, J. Zhang, S. Trolier-McKinstry, J. V. Mantese, R. W. Whatmore, and S. P. Alpay, J. Appl. Phys. 114, 204101 (2013).
- <sup>51</sup> I. B. Misirlioglu, M. T. Kesim, and S. P. Alpay, Appl. Phys. Lett. **105**, 172905 (2014).
- <sup>52</sup>M. Posternak, A. Baldereschi, A. Catellani, and R. Resta, Phys. Rev. Lett. 64, 1777 (1990).
- <sup>53</sup> H. Yin, C. Liu, G.-P. Zheng, Y. Wang, and F. Ren, Appl. Phys. Lett. **114**, 192903 (2019).
- <sup>54</sup>B. Hanrahan, Y. Espinal, C. Neville, R. Rudy, M. Rivas, A. Smith, M. T. Kesim, and S. P. Alpay, J. Appl. Phys. **123**, 124104 (2018).
- <sup>55</sup>K. Coleman, S. Shetty, B. Hanrahan, W. Zhu, and S. Trolier-McKinstry, J. Appl. Phys. **128**, 114102 (2020).
- <sup>56</sup>R. V. K. Mangalam, J. Karthik, A. R. Damodaran, J. C. Agar, and L. W. Martin, Adv. Mater. 25, 1761–1767 (2013).
- <sup>57</sup>J. C. Agar, A. R. Damodaran, M. B. Okatan, J. Kacher, C. Gammer, R. K. Vasudevan, S. Pandya, L. R. Dedon, R. V. K. Mangalam, G. A. Velarde, S. Jesse, N. Balke, A. M. Minor, S. V. Kalinin, and L. W. Martin, Nat. Mater. 15, 549 (2016).
- <sup>58</sup> R. V. K. Mangalam, J. C. Agar, A. R. Damodaran, J. Karthik, and L. W. Martin, ACS Appl. Mater. Interfaces 5, 13235–13241 (2013).
- <sup>59</sup> J. Kim, H. Takenaka, Y. Qi, A. R. Damodaran, A. Fernandez, R. Gao, M. R. McCarter, S. Saremi, L. Chung, A. M. Rappe, and L. W. Martin, Adv. Mater. 31, 1901060 (2019).
- <sup>60</sup> A. Fernandez, J. Kim, D. Meyers, S. Saremi, and L. W. Martin, Phys. Rev. B 101, 094102 (2020).
- <sup>61</sup> F. Y. Lee, S. Goljahi, I. M. McKinley, C. S. Lynch, and L. Pilon, Smart Mater. Struct. 21, 025021 (2012).
- <sup>62</sup> M. Hoffmann, U. Schroeder, C. Künneth, A. Kersch, S. Starschich, U. Böttger, and T. Mikolajick, Nano Energy 18, 154 (2015).
- <sup>63</sup>S. W. Smith, A. R. Kitahara, M. A. Rodriguez, M. D. Henry, M. T. Brumbach, and J. F. Ihlefeld, Appl. Phys. Lett. **110**, 072901 (2017).
- <sup>64</sup>S. Jachalke, T. Schenk, M. H. Park, U. Schroeder, T. Mikolajick, H. Stöcker, E. Mehner, and D. C. Meyer, Appl. Phys. Lett. 112, 142901 (2018).
- <sup>65</sup>C. Mart, T. Kämpfe, S. Zybell, and W. Weinreich, Appl. Phys. Lett. **112**, 052905 (2018).
- 66 J. C. Joshi and A. L. Dawar, Phys. Status Solidi 70, 353-369 (1982).
- <sup>67</sup> A. Hossain and M. H. Rashid, IEEE Trans. **27**, 824–829 (1991).
- <sup>68</sup>D. Shur and G. Rosenman, J. Appl. Phys. **80**, 3445–3450 (1996).
- <sup>69</sup>G. Sebald, L. Seveyrat, D. Guyomar, L. Lebrun, B. Guiffard, and S. Pruvost, Appl. Phys. 100, 124112 (2006).
- <sup>70</sup>G. Sebald, E. Lefeuvre, and D. Guyomar, IEEE Trans. Ultrason., Ferroelectr., Freq. Control 55, 538–551 (2008).
- <sup>71</sup> A. Navid and L. Pilon, Smart Mater. Struct. **20**, 025012 (2011).
- <sup>72</sup>S. Pandya, G. Velarde, L. Zhang, J. D. Wilbur, A. Smith, B. Hanrahan, C. Dames, and L. W. Martin, NPG Asia Mater. 11, 26 (2019).
- <sup>73</sup> R. B. Olsen, D. A. Bruno, and J. M. Briscoe, J. Appl. Phys. 58, 4709-4716 (1985).
- $^{74}\mathrm{B}.$  M. Hanrahan, F. Sze, A. N. Smith, and N. R. Jankowski, Int. J. Energy Res. 41, 1880–1890 (2017).
- <sup>75</sup>G. Sebald, S. Pruvost, and D. Guyomar, Smart Mater. Struct. 17, 015012 (2007).
- <sup>76</sup>G. Rosenman and I. Rez, J. Appl. Phys. **73**, 1904 (1993).
- 77 B. Rosenblum, P. Bräunlich, and J. P. Carrico, Appl. Phys. Lett. 25, 17 (1974).
- <sup>78</sup> J. D. Brownridge, Nature **358**, 287 (1992).
- <sup>79</sup>D.-W. Kim, E. M. Bourim, S.-H. Jeong, and I. K. Yoo, *Physica B* **352**, 200 (2004).
- <sup>80</sup> J. F. Scott, Science **315**, 954 (2007).
- <sup>81</sup> P. C. Fletcher, V. K. R. Mangalam, L. W. Martin, and W. P. King, J. Vac. Sci. Technol., B **31**, 021805 (2013).
- <sup>82</sup>P. C. Fletcher, V. K. R. Mangalam, L. W. Martin, and W. P. King, Appl. Phys. Lett. 102, 192908 (2013).
- 83 S. Das, A. Ghosh, M. R. McCarter, S.-L. Hsu, Y.-L. Tang, A. R. Damodaran, R.
- Ramesh, and L. W. Martin, APL Mater. 6, 100901 (2018).

  84 S. Chen, S. Yuan, Z. Hou, Y. Tang, J. Zhang, T. Wang, K. Li, W. Zhao, X. Liu, L. Chen, L. W. Martin, and Z. Chen, Adv. Mater. 2000857 (2020).
- 85 I. I. Naumov, L. Bellaiche, and H. Fu, Nature 432, 737-740 (2004).

- <sup>86</sup>S. Prosandeev, I. Ponomareva, I. Naumov, I. Kornev, and L. Bellaiche, J. Phys.: Condens. Matter 20, 193201 (2008).
- 87 T. Castan, A. Planes, and A. Saxena, Phys. Rev. B 85, 144429 (2012).
- 88 A. G. Chynoweth, J. Appl. Phys. 29, 563 (1958).
- <sup>89</sup> C.-J. Hus, S. M. Sandoval, K. P. Wetzlar, and G. P. Carman, J. Appl. Phys. 110, 123923 (2011).
- <sup>90</sup> A. Greppmair, N. Galfe, K. Amend, M. Stutzmann, and M. S. Brandt, Rev. Sci. Instrum. 90, 044903 (2019).
- <sup>91</sup> D. Davidovikj, D. J. Groenendijk, A. M. R. V. L. Monteiro, A. Dijkhoff, D. Afanasiev, H. S. J. van der Zant, Y. Huang, E. van Heumen, A. D. Caviglia, and P. G. Steeneken, Nature 3, 163 (2020).
- <sup>92</sup>Y. Ivry, V. Lyahovitskaya, I. Zon, I. Lubomirsky, E. Wachtel, and A. L. Roytburd, Appl. Phys. Lett. **90**, 172905 (2007).
- <sup>93</sup>S. Lisenkov, B. K. Mani, J. Cuozzo, and I. Ponomareva, Phys. Rev. B **93**, 064108 (2016).
- <sup>94</sup>Y. Liu, I. C. Infante, X. Lou, L. Bellaiche, J. F. Scott, and B. Dkhil, Adv. Mater. 26, 6132–6137 (2014).
- <sup>95</sup> H. Khassaf, T. Patel, R. J. Hebert, and S. P. Alpay, J. Appl. Phys. **123**, 024102 (2018).
- <sup>96</sup>D. Pesquera, E. Parsonnet, A. Qualls, R. Xu, A. J. Gubser, J. Kim, Y. Jiang, G. Velarde, Y. L. Huang, H. Y. Hwang, R. Ramesh, and L. W. Martin, Adv. Mater. 32, 2003780 (2020).
- <sup>97</sup>R. A. Kishore and S. Priya, Materials 11, 1433 (2018).
- <sup>98</sup>S. Lee, R. H. T. Wilke, S. Trolier-McKinstry, S. Zhang, and C. A. Randall, Appl. Phys. Lett. **96**, 031910 (2010).
- S. Lee, S. Dursun, C. Duran, and C. A. Randall, J. Mater. Res. 26, 26–30 (2011).
   S. Lee, J. A. Bock, S. Trolier-McKinstry, and C. A. Randall, J. Eur. Ceram. Soc. 32, 3971–3988 (2012).

- <sup>101</sup> A. Banik, T. Ghosh, R. Arora, M. Dutta, J. Pandey, S. Acharya, A. Soni, U. V. Waghmare, and K. Biswas, Energy Environ. Sci. 12, 589 (2019).
- <sup>102</sup>D. Sarkar, T. Ghosh, S. Roychowdhury, R. Arora, S. Sajan, G. Sheet, U. V. Waghmare, and K. Biswas, J. Am. Chem. Soc. 142, 12237–12244 (2020).
- <sup>103</sup>D. Wu, L. Xie, X. Xu, and J. He, Adv. Funct. Mater. **29**, 1806613 (2019).
- <sup>104</sup>P. E. Hopkins, C. Adamo, L. Ye, B. D. Huey, S. R. Lee, D. G. Schlom, and J. F. Ihlefeld, Appl. Phys. Lett. **102**, 121903 (2013).
- <sup>105</sup>J. F. Ihlefeld, B. M. Foley, D. A. Scrymgeour, J. R. Michael, B. B. McKenzie, D. L. Medlin, M. Wallace, S. Trolier-McKinstry, and P. E. Hopkins, Nano Lett. 15, 1791–1795 (2015).
- <sup>106</sup>C. Liu, Y. Chen, and C. Dames, Phys. Rev. Appl. 11, 044002 (2019).
- <sup>107</sup>B. Hanrahan, C. Neville, A. Smith, N. Ter-Gabrielyan, N. Jankowski, and C. M. Waits, Adv. Mater. Technol. 1, 1600178 (2016).
- <sup>108</sup>B. Hanrahan, J. Easa, A. Payne, Y. Espinal, S. P. Alpay, H. Kareem, C. O'Brien, and A. Smith, Cell Rep. Phys. Sci. 1, 100075 (2020).
- <sup>109</sup>R. B. Olsen and D. D. Brown, Ferroelectrics **40**, 17–27 (1982).
- <sup>110</sup>D. Zakharov, B. Gusarov, E. Gusarova, B. Viala, O. Cugat, J. Delamare, and L. Gimeno, J. Phys.: Conf. Ser. 476, 012021 (2013).
- <sup>111</sup>I. M. McKinley, F. Y. Lee, and L. Pilon, Appl. Energy **126**, 78–89 (2014).
- <sup>112</sup>H. Khassaf, T. Patel, and S. P. Alpay, J. Appl. Phys. **121**, 144102 (2017).
- <sup>113</sup>J.-H. Lee, K. Y. Lee, M. K. Gupta, T. Y. Kim, D.-Y. Lee, J. Oh, C. Ryu, W. J. Yoo, C.-Y. Kang, S.-J. Yoon, J.-B. Yoo, and S.-W. Kim, Adv. Mater. 26, 765–769 (2014).
- 114Y. Yang, H. Zhang, G. Zhu, S. Lee, Z.-H. Lin, and Z. L. Wang, ACS Nano 7, 785–790 (2013).
- <sup>115</sup>B. Hanrahan, Y. Espinal, S. Liu, Z. Zhang, A. Khaligh, A. Smith, and S. P. Alpay, J. Mater. Chem. C 6, 9828–9834 (2018).